The effect of fo2 source on the solubility, diffusion, and speciation of tin in haplogranitic melt at 850°C and 2 kbar

Robert L. Linnen, Michel Pichavant, Holtz François, Simon Burgess

Pergamon

Geochimica et Cosmochimica Acta, Vol. 59, No. 8, pp. 1579–1588, 1995

0016-7037/95 $9.50 + .00

0016-7037(95)00064-X

The effect of f_{O_2} on the solubility, diffusion, and speciation of tin in haplogranitic melt at 850°C and 2 kbar

ROBERT L. LINNEN,[1,*] MICHEL PICHAVANT,[1] FRANÇOIS HOLTZ,[1] and SIMON BURGESS[2,†]

[1]Centre de Recherche sur la Synthèse et Chimie des Minéraux, Centre National de Recherche Scientifique, 1A rue de la Férollerie, 45071 Orléans cedex 2, France

[2]Department of Geography and Geology, University of St. Andrews, St. Andrews, Fife KY16 9ST, Scotland, UK

(*Received January* 18, 1994; *accepted in revised form January* 13, 1995)

Abstract—Diffusion profiles of tin were produced in hydrous silicate melts adjacent to cassiterite crystals; the method of Harrison and Watson (1983) was adapted to produce Sn diffusion profiles in hydrous silicate melts adjacent to cassiterite crystals at 2 kbar, 850°C, and various redox conditions, from which information on the solubility, diffusion, and speciation of Sn in silicate liquids can be obtained. The use of diffusion profiles and a hydrous, yet slightly H_2O-undersaturated melt composition were chosen, in order to avoid the loss of Sn to the noble-element capsule walls. Such losses occurred at reduced conditions in the previous experimental studies on the solubility or partitioning of Sn in silicate liquids (±fluid phase), which probably interfered with the redox or SnO_2 activity control of those experiments.

The redox conditions investigated in this study were controlled by the intrinsic or an imposed f_{H_2} in rapid-quench cold-seal and internally heated pressure vessels, and were measured by either the hydrogen sensor or Shaw membrane techniques. Cassiterite solubilities at 850°C and 2 kbar range from 28,000 ppm SnO_2 at FMQ−0.84 to approximately 800 ppm at FMQ+3.12, in a haplogranitic melt with a normative (anhydrous) composition of 37.2% quartz, 28.3% orthoclase, 34.1% albite, 0.4% corundum, and 5.6 wt% H_2O. For redox conditions higher than FMQ+1.5, SnO_2 solubility is independent of f_{O_2}, indicating that cassiterite dissolved into the melt largely as Sn^{4+}. By contrast at more reduced conditions, log SnO_2 concentration vs. log f_{O_2} define a slope of approximately −0.5, implying that Sn is dominantly in the 2^+ valence, if γSn^{2+}_{melt} is constant. The solubilities obtained at reduced conditions in this study are an order of magnitude higher than previously published data (at a comparable *P-T*, composition and f_{H_2} of the autoclave); the low values in the previous work are attributed to the loss of Sn to the capsule walls. The diffusion of Sn is also apparently related to f_{O_2}, ranging from approximately 10^{-8} cm²/s at FMQ-0.84 to 10^{-9} cm²/s at FMQ+3.12. This is consistent with Sn^{2+} behaving as a network modifier, whereas the diffusion of Sn^{4+} is slower, similar to other high field strength elements. The strong f_{O_2} dependence of Sn solubility can be used to explain some magmatic tin deposits and also indicates that tin might prove useful as a marker of redox changes of a variety of magmatic systems.

INTRODUCTION

The vast majority of Sn deposits are associated with granitic rocks, thus, a great deal of research has been devoted to the petrogenesis of these granites. In order for Sn to be sufficiently concentrated to crystallize cassiterite either at supersolidus (e.g., Linnen et al., 1992) or subsolidus (e.g., Jackson et al., 1982) conditions, it is generally believed that the granitic melts must have evolved under reduced conditions (e.g., Ishihara, 1981; Lehmann, 1990). In spite of the proposed dependency of Sn behaviour on oxygen fugacity, very few experiments have been conducted on the effect of f_{O_2} on Sn solubility in granitic melts and most SnO_2 solubility studies were conducted at oxidized conditions (see the review in Štemprok, 1990). Naski and Hess (1985) investigated the effects of melt composition and f_{O_2} on Sn solubility in dry granitic glasses at 1 atm. and concluded that, for the conditions examined (f_{O_2} > Ni-NiO), f_{O_2} has no effect on Sn solubility. The fact that the experiments were conducted dry, at 1 atm., and at oxidized conditions limits their applicability to natural tin granite petrogenesis.

The most comprehensive study of Sn solubility in granitic liquids to date is that of Taylor and Wall (1992). SnO_2 concentrations were determined in silicate melts and aqueous fluids coexisting with cassiterite and the results indicate that f_{O_2} (over the range FMQ−1 to FMQ+1.4), along with melt composition, is an important control of cassiterite solubility in haplogranitic liquids. The experimental method (similar to most other work) consisted of sealing cassiterite crystals, silicate gel, and H_2O (±NaCl) in Au capsules, with a large aqueous fluid to silicate melt ratio. The dissolution of tin into the vapor phase, and consequent rapid transport and loss of Sn by alloying with the capsule (e.g., M. Pichavant and D. A. C. Manning, unpubl. data; Keppler and Wyllie, 1991) was not considered to interfere with the solubility of tin in silicate liquids.

In this study, we have eliminated the problem of Sn forming an alloy with noble elements used as containers, while maintaining accurate control of redox conditions. The experimental method of Harrison and Watson (1983) was adapted to measure diffusion profiles of SnO_2 away from cassiterite crystals at fixed oxygen fugacities, from which information on the solubility, diffusivity, and structure of Sn in haplogranite melt

* *Present address:* Bayerisches Geoinstitut, Universitat Bayreuth, D-95440 Bayreuth, Germany.

† *Present address:* Department of Geology and Geophysics, The University of Edinburgh, Edinburgh EH9 3JW, Scotland, UK.

can be obtained. In contrast with many other studies (e.g., Webster and Holloway, 1988; Taylor and Wall, 1992), where the interaction of melt and excess water (or fluid phase) causes modifications of the melt composition, SnO_2 solubility in this study was determined in a hydrous, yet slightly H_2O-undersaturated melt; thus, the problems of changes in melt composition and the loss of Sn by alloying were both avoided. Given that the solubility of a variety of other metals is f_{O_2} dependent and that many of these metals also form alloys with Au, Pt, etc., the method employed here, potentially, has further applications in experimental petrology.

EXPERIMENTAL AND ANALYTICAL METHODS

Equipment

All the experiments were conducted at approximately 850°C and 2 kbar (see Table 1), using three types of autoclaves (each with a different intrinsic f_{H_2}): an internally heated pressure vessel (IHPV) working horizontally, a rapid-quench cold-seal pressure vessel working horizontally, and an IHPV equipped with a modified Shaw membrane and operated vertically (Scaillet et al., 1992). The first two autoclaves were pressurized by Ar, whereas the vertical IHPV was pressurized by Ar-H_2 mixtures. In the latter, 0.5–14 bars of H_2 was first loaded, depending on the desired final H_2 fugacity, followed by approximately 1000 bars of Ar. Chromel-alumel thermocouples, calibrated against NaCl melting at 1 and 2000 bars, were employed in all three autoclaves and the accuracy of the temperature measurements are better than ±10°C. Total pressures in the two IHPV vessels were measured with transducers, calibrated against Heise Bourdon tube gauges and in the rapid-quench vessel was measured directly with a Bourdon gauge, with an error of ±20 bars in each of the autoclaves. Hydrogen fugacities in the vertical IHPV experiments were measured with Protais tube gauges with accuracies of ±1.0 bar at $f_{H_2} > 10$ bar and ±0.1 bar at $f_{H_2} < 10$ bar. Heating durations depend on the autoclave and are about 0.5 h for the rapid-quench and vertical IHPV and 2 h for the horizontal IHPV.

TABLE 1. Experimental conditions and results.

STAGE I

Exp.	Autoclave	f_{H_2}	t	wt% H_2O	P	T	log f_{O_2}melt
Sn1	VIHPV	44	96	5.65	2313	849	-14.12
Sn2-1	VIHPV	31	33	5.68	2243	848	-13.85
Sn2-2	VIHPV	31	33	5.68	2243	848	-13.85
Sn2-3	VIHPV	31	33	5.68	2243	848	-13.85
Sn3	HIHPV	2.3	94	5.63	2022	856	-11.47
Sn4	CSRQ	0.5	84	5.64	2000	850	-10.28
Sn5	VIHPV	21	54	5.67	2140	854	-13.40
Sn6	VIHPV	28	72	5.65	2138	858	-13.56
Sn7	VIHPV	13	72	5.35	2147	858	-12.95
Sn11	VIHPV	2.5	48	5.56	2313	856	-11.47
Sn12	VIHPV	46	72	5.37	2147	854	-14.13
C2-1	VIHPV	23.3	55	7.12	2120	850	-13.51
C2-2	VIHPV	23.3	55	7.12	2120	850	-13.51

STAGE II

						Solubility log ppm SnO_2			-log D cm^2/sec		
Exp	P	T	t	logf_{O_2}	ΔFMQ	ave.	max.	min.	ave.	max.	min.
Sn1	2179	851	6.25	-14.10	-0.74	4.29	4.39	4.13	7.87	7.44	8.09
Sn2-1	2243	854	5.0	-13.71	-0.42	4.24	4.33	4.22	-	-	-
Sn2-2	2243	854	5.0	-13.71	-0.42	4.27	4.31	4.25	-	-	-
Sn2-3	2232	855	3.0	-13.69	-0.42	4.25	4.30	4.18	7.91	7.63	8.21
Sn3	2030	849	4.0	-11.62	1.79	2.85	2.90	2.70	8.99	8.57	9.30
Sn4	2000	849	3.5	-10.29	3.12	2.90	3.11	2.70	8.03	7.83	8.47
Sn5	2137	852	6.0	-13.44	-0.10	3.99	4.02	3.94	7.89	7.61	8.19
Sn6	2125	858	6.25	-13.57	-0.35	4.20	4.28	4.15	7.94	7.51	8.22
Sn7	2162	859	6.0	-12.93	0.27	3.75	3.81	3.69	8.01	7.90	8.14
Sn11	2175	851	6.0	-11.62	1.74	2.95	3.04	2.90	8.34	8.19	8.52
Sn12	2058	852	6.0	-14.19	-0.84	4.45	4.50	4.42	7.75	7.38	7.99
C2-1	2060	853	6.0	-13.47	-0.17	4.21	4.22	4.19	8.08	7.99	8.19
C2-2	2010	855	24.0	-13.44	-0.18	4.19	4.23	4.15	8.22	8.17	8.26

Abbreviations: VIHPV, internally-heated pressure vessel operated vertically; HIHPV, internally-heated pressure vessel operated horizontally; CSRQ, cold-seal rapid-quench autoclave, f_{H_2} is the H_2 fugacity in bars; t, experimental run duration in hours; wt% is the weight % H_2O loaded into the capsule, in the case of experiment C2 there is an excess of water; P, total pressure in bars; T, temperature in °C; ΔFMQ, departure of logf_{O_2} from the FMQ buffer, calculated at the P and T of the experiment (Chou, 1978). The f_{O_2}melt was calculated using a_{H_2O} after Burnham (1979), $f^*_{H_2O}$ from Haar *et al.* (1984), water formation constant from Robie *et al.* (1978) and the average anhydrous composition of glass >500 μm from cassiterite, in wt%: K_2O 4.78, Na_2O 4.04, Al_2O_3 12.24 and SiO_2 78.94.

Starting Materials

Since f_{O_2} was intended to be the only variable, the experiments were largely carried out using a single melt composition. A dry gel or glass from the study of Holtz et al. (1992a; Glass no. $3_5 33_5$) was used as a starting material for all but two experiments. Its normative composition, determined in this study by electron microprobe analyses of hydrous glasses (discussed below) is 37.2% quartz, 28.3% orthoclase, 34.1% albite, and 0.4% corundum, which agrees well with the anhydrous analysis given by Holtz et al. (1992a) (see Table 2). This composition is very close to that of the 2 kbar H_2O-saturated haplogranite minimum and its water solubility is well known (5.8 wt% at 850°C and 2 kbar; Holtz et al., 1992b). The depletion of the starting gel during the course of this study necessitated the use of a similar composition for two experiments. The second composition is slightly peralkaline, with a normative composition of 35.3% quartz, 26.2% orthoclase, 38.0% albite, and 0.5% sodium metasilicate. The source of cassiterite was synthetic monocrystals (>99% SnO_2) from the study of Thiel and Helbig (1976).

Experimental Method and Products

The experiments were run in two stages. In the first stage distilled H_2O was loaded into an Au capsule (i.d. 4.8 mm, o.d. 5.2 mm, length 2.0–4.0 cm), followed by the haplogranite gel or glass, and sealed by arc welding. The capsules were checked for weight loss after welding, then again after storage in a drying oven at 110°C for at least 8 h. The storage also helped to evenly distribute the water in the capsule, which facilitated making a homogeneous melt. The amount of added water was such that the melt contained roughly 5.6 wt% H_2O (Table 1), which is slightly H_2O-undersaturated for the P-T conditions of this study (Holtz et al., 1992b); thus, the activity of water in the melt (a_{H_2O}) is nearly one, yet the problem transport of Sn to the capsule via a vapor phase is avoided. In the case of the second composition, the value of water saturation is less certain. Therefore, an excess of H_2O (7 wt%) was initially loaded into the capsule.

The duration of the first stage was two to four days, in order to produce a homogeneous glass and to establish the f_{H_2}. After checking for weight loss, the glass in the unopened capsule was crushed using pliers. The capsule was opened and glass fragments were loaded into a fresh Au capsule, approximately 1 cm long and closed at the base with a triangular weld. A single cassiterite crystal (approximately 0.5 × 1.0 × 2.0 mm) was then placed in the centre of the glass fragments and the capsule was crimped and welded shut. During the second stage, the capsule loaded with cassiterite was placed in the same autoclave and re-exposed to the same P_{total}-T-f_{H_2} conditions, generally for 6 h, but ranging from 3 to 24 h. Using this method, the dissolution of SnO_2 occurred at fixed P-T-redox conditions. After quenching (maximum of a few minutes), the capsules from stage two were weighed, then cut perpendicular to the tabular cassiterite crystal. This enabled analysis of tin in the glass adjacent to the crystal and in the Au capsule. The experimental products were always glass + cassiterite, consistent with the haplogranite liquidus temperature in Holtz et al. (1992a).

Different run durations (3–5 h) and the use of Au and Pt capsules were compared in the second stage of experiment Sn2, and run durations of 6 and 24 h were compared in experiment C2 (Table 1). It is also important to note that cassiterite is stable at log oxygen fugacities as low as approximately FMQ−1.5 at 850°C and 2 kbar (Robie et al., 1979; Johnson et al., 1992); the most reduced experiment in this study was at FMQ−0.84, thus, cassiterite was the stable Sn-O phase in all experiments.

Determination of f_{O_2}

The intrinsic oxygen fugacities of the rapid-quench and horizontal IHPV were determined by the hydrogen sensor technique (Chou, 1978), with an accuracy of better than ±0.5 log units. During the vertical IHPV experiments, the diffusion of H_2 into the Shaw membrane is restricted to the hot-zone in the autoclave and H_2 fugacity around the Au capsule was measured directly with a Protais tube gauge (Scaillet et al., 1992). The time required to reach osmotic equilibrium between the Protais tube gauge and autoclave, via the Shaw membrane and H_2 line, was typically 24 h, thus, hydrogen fugacities were only determined during the first stage of each experiment. However, the rate of equilibration of hydrogen across the Au capsule is on the order of minutes at 850°C (Scaillet et al., 1992), therefore the f_{H_2} determined in stage 1 was also applied to stage 2, given that the initial P_{H_2} (at 25°C), T, and P_{total} (at run conditions) were identical.

The activity of water (a_{H_2O}) was estimated from the water content of the melts (determined during the loading of the capsules), the melt composition (determined from electron microprobe analyses), and the activity-composition model of Burnham (1979). Using this activity and the value of $f_{H_2O}^{pure}$, calculated at P-T from the equations of Haar et al. (1984), the fugacity of H_2O was estimated from:

$$a_{H_2O}^{melt} = f_{H_2O}^{melt} / f_{H_2O}^{pure}. \quad (1)$$

Finally, using $f_{H_2O}^{melt}$ ($f_{H_2}^{melt} = f_{H_2}^{Ar\text{-}H_2}$) and $f_{H_2O}^{melt}$, the f_{O_2} was calculated using the dissociation constant of water, from Robie et al. (1979):

$$\log K_w = \log f_{H_2O} - \log f_{H_2} - 0.5 \log f_{O_2}. \quad (2)$$

The equations of Burnham (1979) predict water saturation of the melt for composition, P, and T considered here, at 6.0 wt% H_2O, which is slightly in excess of the 5.8 wt% from the experiments of Holtz et al. (1992b). We have assumed that the model of Burnham

TABLE 2. Average glass compositions 20 and >500 μm from cassiterite monocrystals.

	electron microprobe analyses				normative compositions			
Exp.	K_2O	Na_2O	SiO_2	Al_2O_3	Q	Or	Ab	C
Sn2-3	4.57	3.51	79.33	12.58	41.4	27.0	29.7	1.9
Sn4	4.84	3.95	78.93	12.27	37.4	28.6	33.4	0.5
Sn5	4.72	3.86	79.44	11.97	38.9	27.9	32.7	0.5
Sn6	4.80	3.75	79.18	12.28	39.0	28.4	31.7	0.9
Sn7	4.73	3.74	79.58	11.95	39.7	28.0	31.7	0.7
Sn11	4.78	4.01	78.99	12.22	37.4	28.3	33.9	0.5
Sn12	4.63	3.38	79.50	12.49	42.1	27.4	28.6	1.9
>500 μm	4.78	4.03	78.89	12.24	37.2	28.3	34.1	0.4
Holtz	4.77	3.96	78.74	12.53	37.5	28.2	33.9	0.8

Abbreviations are Q, quartz; Or, orthoclase; Ab, albite; C, corundum. Compositions are normalized to 100%. For each experiment the average is taken from analyses 20 μm from cassiterite. For >500 μm, the average composition >500 μm from cassiterite in each experiment was calculated first, then these values were used to calculate the average Sn-free composition. Holtz is the anhydrous composition given by Holtz *et al.* (1992a) for the same glass.

(1979) is still valid in the presence of small amounts of H_2 dissolved the silicate liquid (cf. Persikov et al., 1990). An additional consideration is that at reduced conditions, the dissolution of the cassiterite crystal produces oxygen, which presumably combines with hydrogen dissolved in the melt, and could have increased the water content at the mineral-melt interface. The maximum amount of water produced can be estimated by the SnO_2 concentration in the glass at the cassiterite interface and the reaction:

$$SnO_2(\text{crystal}) + H_2(\text{melt}) = SnO(\text{melt}) + H_2O(\text{melt}). \quad (3)$$

In the most reduced experiment (Sn12), this reaction could have increased the water content of the melt by up to 0.3 wt% H_2O at the crystal-melt interface. This reaction neglects the Sn^{4+}(melt) component of dissolution and the fact that the newly formed H_2O should diffuse in a compositional gradient. Nevertheless, the redox reaction of cassiterite dissolution could have increased the water content at the crystal-melt interface. This, together with the fact that the equations slightly overestimate H_2O solubility suggest that the a_{H_2O} values calculated after Burnham (1979), result in a minimum estimate of f_{O_2}. By contrast, the maximum f_{O_2} is calculated by assuming water saturation; these values are less than 0.1 log units higher (except experiment Sn11, 0.135 higher) than those reported in Table 1. It is important to note that the diffusion of H_2 in granitic melts is 2–3 orders of magnitude faster than that of H_2O (Persikov et al., 1990); thus, while f_{O_2} may have increased slightly as a result of higher a_{H_2O}, f_{H_2} remained constant. Since a_{H_2O} is pressure and temperature dependent, it is more convenient to compare the redox conditions of the different experiments to a solid buffer. We have chosen the fayalite-magnetite-quartz buffer (FMQ) as a reference and the redox conditions of this study range from FMQ−0.84 to FMQ+3.12 (Table 1). The effect of minor differences in *P-T* between stages 1 and 2 have also been considered; these are calculated to have been, at worst, a log f_{O_2} difference of 0.16 (Table 1), and given the fast diffusion of H_2 in silicate melts, is not considered to be a significant error. It is also obvious that both cassiterite and water dissociation are redox reactions. For the diffusion profiles in this study, the amount of water produced by reaction 3 is at most, two orders of magnitude lower than the water content of the melt. Therefore f_{O_2} will be imposed by the f_{H_2} and f_{H_2O} of the melt, rather than by SnO_2 dissolution (discussed further below).

For the slightly peralkaline composition (C2), the 110 bar difference in total pressure between the first and second stages (Table 1) likely resulted in vapor saturation. However, the mass of excess water, <1 mg, was not sufficient to interfere with the diffusion experiment or to transport tin to the capsule walls.

Analytical Methods

Tin contents were determined with a CAMECA SX-50 electron microprobe at the CNRS-BRGM-UO laboratory in Orléans using a SnO_2 standard and the PAP correction program. Various operating conditions were tried and statistical analyses of the errors and detection limits were calculated using the method of Ancey et al. (1978). Optimal conditions were found to be 20 kV, 50 nA, 60–150 s counting times and a beam width of 1 μm, with an error of ±100 to ±200 ppm at 95% confidence. Although volatiles are lost during analysis using these conditions, Sn contents determined with high and low currents and short and long counting times were comparable within the error limits, indicating that such volatilization did not affect the analysis of Sn. For each experiment, a minimum of four SnO_2 profiles were obtained, using increments of 10 or 20 μm. A blank standard, consisting of a cassiterite monocrystal and Sn-free glass from stage 1, was also prepared to test for possible interference from cassiterite. Tin could not be detected (<100 ppm) in glass 50 μm from the cassiterite crystal (the thickness of the resin between the cassiterite and the glass); therefore, fluorescence from cassiterite is not considered to be an analytical problem.

Separate major-element profiles using the CAMECA SX-50 electron microprobe and PAP correction program were obtained parallel to the Sn profiles, over increments of 20–100 μm. The operating conditions were 15 kV, 6 nA, 6 s counting times for Na_2O and K_2O and 10 s counting times for Al_2O_3 and SiO_2 with a beam width of 15 μm. The Na_2O and K_2O contents were subsequently corrected by factors of 1.07–1.08 and 0.98–0.99, respectively, using a secondary hydrous glass standard (with Na_2O and K_2O contents determined by wet chemical analysis) that was analysed several times during the same session as the major-element profiles (cf. Pichavant, 1987). The precision of the analyses of the glass standard, and hence, the experimental glasses, is approximately 5% relative for Na_2O and K_2O, 4% relative for Al_2O_3, and 1% relative for SiO_2.

RESULTS

Cassiterite Solubility

After SnO_2 concentration profiles in glasses adjacent to cassiterite monocrystals were determined by electron microprobe analyses, cassiterite solubilities were calculated using the method of Harrison and Watson (1983), by inverting the error function of diffusion from an infinite planar source. The calculated SnO_2 concentration at the cassiterite-glass interface is the cassiterite solubility. To remove the bias of equal weighting being given to samples with low concentration, values of <10% of the SnO_2 solubility were excluded from the calculation (Rapp and Watson, 1986). An example of SnO_2 profiles and a linearized form of the error function, determined for experiment Sn5, is given in Fig. 1. The fact that the error function essentially intersects the origin (Fig. 1b) is evidence that the crystal did not retreat significantly during the exper-

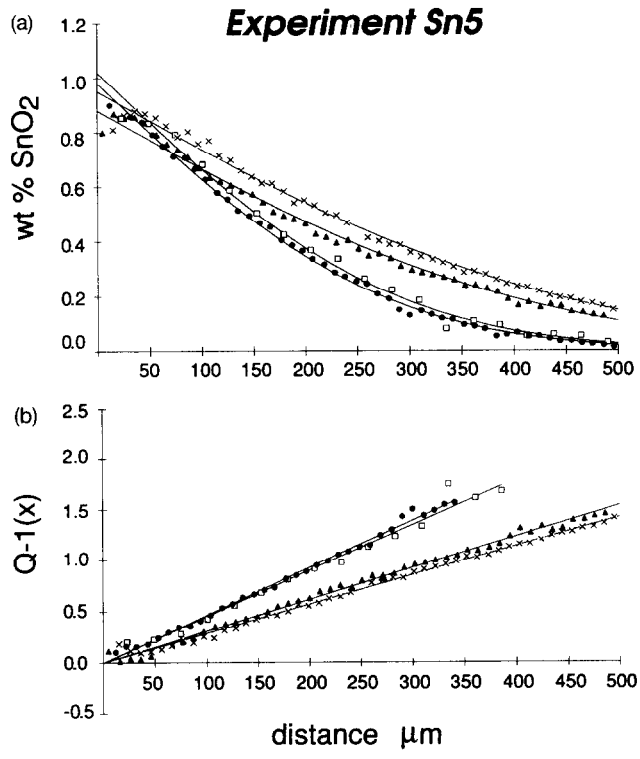

FIG. 1. Diffusion profiles of tin concentration (reported as SnO_2) in haplogranite glass adjacent to the cassiterite monocrystal in experiment Sn5. (a) Results of electron microprobe traverses. The different symbols represent different traverses away from the same cassiterite crystal and the solid lines are the calculated diffusion profiles for each case. (b) A linearized form of the error function for the profiles in Fig. 1a. The good correlation between the fit (solid lines) and the data (symbols) and the intersection at the origin indicate that the chosen model (infinite planar diffusion without significant resorption of the crystal) is valid.

iment and the excellent agreement of the analyses with the calculated diffusion profiles indicates that the assumed diffusion model is valid (Harrison and Watson, 1983). It is important to note that the shape of the diffusion profiles on Fig. 1 vary, but the solubility remains constant. This most likely results from the polished section not being exactly perpendicular to the cassiterite crystal and errors in estimating distances result in variations in the calculated diffusion coefficients but not in the solubilities.

The experimental results of SnO_2 solubility are summarized in Table 1 and Fig. 2. It is clear that cassiterite solubility is strongly dependent on f_{O_2}, ranging from approximately 800 ppm at a log f_{O_2} value of >FMQ+1.5, to 28,000 ppm at a log f_{O_2} value of FMQ−0.84. Tin diffused into the capsule wall in only one case (Sn1). Because the experiment was H_2O-undersaturated, this diffusion was restricted to a single point where the cassiterite crystal touched the capsule wall thus the solubility determined from this experiment is probably reasonable. However, it is interesting to note that SnO_2 solubility from this experiment lies slightly below the trend defined by the other reduced experiments (FMQ−0.84 to FMQ+0.27) and that the uncertainty is greater (Fig. 2). Cassiterite solubility is slightly higher in the weakly peralkaline C2 composition (open squares in Fig. 2), consistent with the effect of increasing the melt alkali/Al ratio on SnO_2 solubility observed in other studies, e.g., Naski and Hess (1985), but a detailed investigation of this effect is beyond the scope of this paper.

In experiments Sn2-1 and Sn2-2, the use of Au and Pt capsules, respectively, were compared. The consistency of the solubilities (1.7 ± 0.4 and 1.9 ± 0.2 wt%, respectively; Table 1) confirms the absence of alloying problems between tin and the noble elements used as containers. Hydrogen diffusion is faster in Pt than in Au capsules (Chou, 1978); however at the conditions of this study, H_2 diffusion is sufficiently rapid (see above), hence, Au capsules were retained for all other experiments. It has to be noted that the solubility was calculated assuming that the major-element composition of the melt was constant (i.e., only Sn diffused). This is not the case in all our experiments.

Compositional Variation

Because cassiterite solubility is dependent on the alkali/Al ratio of the melt (Naski and Hess, 1985; Taylor and Wall, 1992), major-element profiles were measured parallel to the tin profiles (Table 2). For f_{O_2} conditions were cassiterite solubility is less than approximately 1 wt% SnO_2, no variations of composition with distance from the cassiterite monocrystal are apparent. However, at higher SnO_2 solubilities, compositional variation can be detected. Figure 3 shows the compositional variation in the most reduced experiment (Sn12). A representative SnO_2 traverse and the calculated diffusion profile are shown in Fig. 3a. Note that the analysis closest to the cassiterite monocrystal lies below the diffusion profile; this is characteristic of solubilities greater than approximately 1.5 wt% SnO_2. In order to determine whether or not major-elements diffused during the second stage of the experiment, the effect of SnO_2 dilution must be taken into account (i.e., normalized to SnO_2-free). Each major element, at a given distance from the cassiterite monocrystal, was, therefore, adjusted by the wt% SnO_2, taken from the diffusion profile (e.g., for analyses of 3.0 wt% Na_2O and 2.0 wt% SnO_2, the adjusted Na_2O is 3.06 wt%). It is clear that in experiment Sn12, Na_2O moved away from the cassiterite monocrystal during the dissolution of SnO_2 (Fig. 3b). By contrast, movement of K_2O, SiO_2 (Fig. 3c,d) and Al_2O_3 (not shown) cannot be demonstrated within the precision of the electron microprobe. However, in a few other major-element traverses (in reduced experiments), some K_2O apparently diffused, in addition to

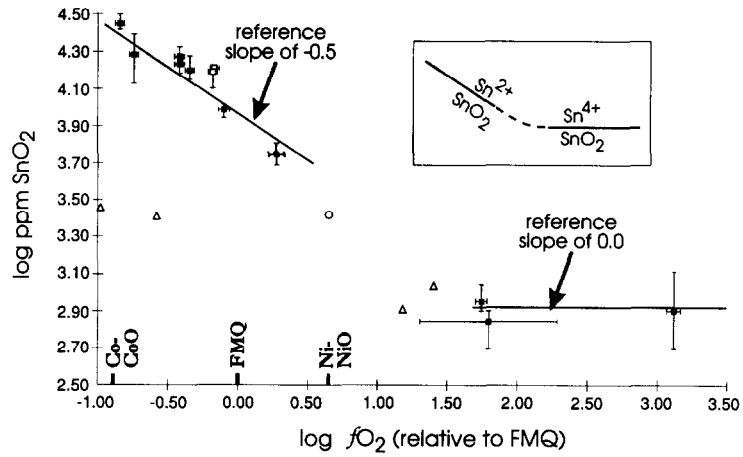

FIG. 2. Log solubility of tin (reported as ppm SnO_2) vs. log f_{O_2} in haplogranitic melts. The solid squares represent the average solubilities determined in this study for the peraluminous composition and the open squares for the weakly peralkaline composition. The vertical error bars represent the range of solubilities calculated from different diffusion profiles, whereas the horizontal error bars represent either the error in the f_{H_2} measurement in the case of the vertical IHPV experiments or the range of f_{H_2} determined by the hydrogen sensor technique for the horizontal IHPV and cold-seal rapid-quench experiments. The open triangles represent the solubilities determined by Taylor and Wall (1992) and the open circle is from Ryabchikov et al. (1978). The inset shows part of the phase equilibria in the system Sn–O in terms of activity of SnO_2 vs. activity of O_2.

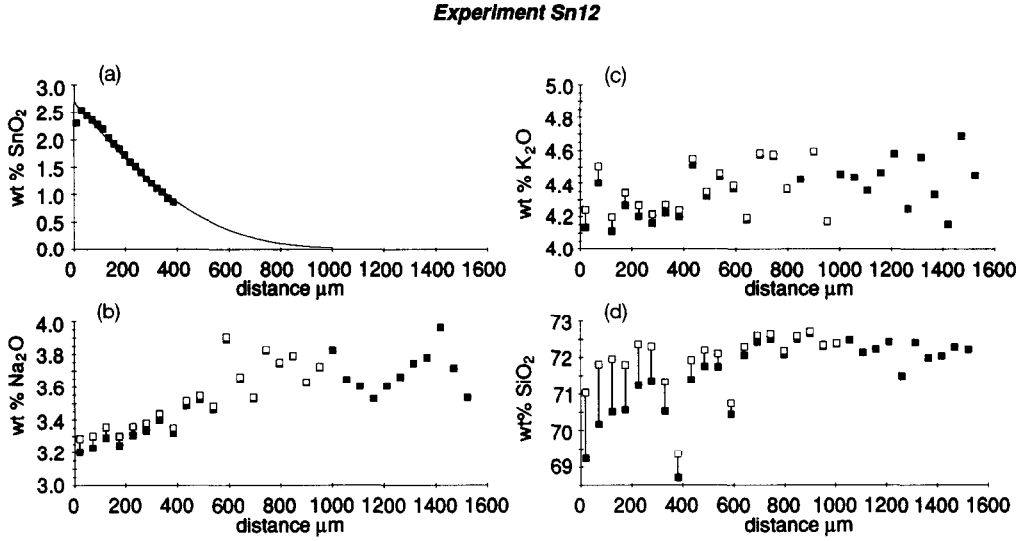

FIG. 3. Representative electron microprobe analyses of SnO_2 and major elements a function of distance from the cassiterite monocrystal in experiments Sn12 (the most reduced experiment). (a) SnO_2 analyses (solid squares) and the calculated diffusion profile (solid line). (b–d) Na_2O, K_2O, and SiO_2 analyses, respectively (solid squares), and concentrations normalized to a Sn-free composition (open squares). At distances > 1000 μm from the cassiterite crystal, the normalization is not required.

Na_2O. The diffusion of Na_2O, and probably K_2O, is also evident on Table 2, where major-element averages at a distance of 20 μm from the cassiterite monocrystals in most of the experiments are compared to the Sn-free compositions (taken as >500 μm from the cassiterite monocrystals). For example, in experiments Sn2-3 and Sn12 the log SnO_2 solubility is 4.25 and 4.45 ppm, respectively, and the loss of alkalis at the cassiterite-glass contact has resulted in an increase of the normative corundum content to 1.9 wt% (calculated for an anhydrous SnO_2-free composition). By contrast, in experiments Sn4, 5, 7, and 11 the log SnO_2 solubility is <4.0 ppm and the normative corundum contents range from 0.5 to 0.7 wt%, which can be considered to be the same as the starting composition, within the error limit of the analysis. It is important to establish whether this alkali diffusion affected cassiterite solubility, although it is also important to note that the 1.3 wt% increase in normative Al_2O_3 in this study is less than the compositional variation observed in experiments that use high fluid to melt ratios, e.g., Taylor and Wall (1992).

If the method employed in this study is valid, Sn diffusivities and solubilities should be independent of time, i.e., if alkali diffusion or redox control are significant problems, the calculated cassiterite solubility would appear to be time-dependent. The effect of time was, therefore, examined in two sets of experiments at high f_{H_2}, since alkali diffusion was only detected at these conditions. A diffusion time of 3 h (Sn2-3) vs. 5 h (Sn2-1 and Sn2-2) at log f_{O_2} of FMQ−0.42 did not produce a change in the solubility of cassiterite (1.8 ± 0.3 and 1.8 ± 0.4 wt% SnO_2, respectively, Table 1). In order to compare longer run times, the second composition had to be

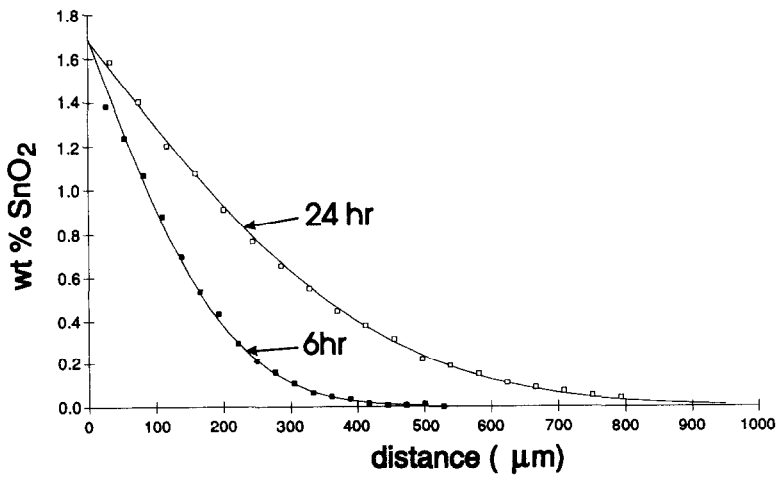

FIG. 4. Representative diffusion profiles for experiment C2-1 (6 h) and C2-2 (24 h) illustrating that for the time variation considered, cassiterite solubility is not time dependent.

used. In this case, a diffusion time of 6 h (C2-1) vs. 24 h (C2-2) at log f_{O_2} of FMQ−0.11 did not produce a change in the solubility of cassiterite (1.6 ± 0.1 and 1.5 ± 0.2 wt% SnO_2, respectively, Table 1). Two diffusion profiles from the latter experiment are shown on Fig. 4 and it is clear that for both 6 and 24 h, the observed profiles closely match infinite planar diffusion (solid lines on Fig. 4). The use of diffusion profiles to calculate solubilities is thus justified by the fact that cassiterite solubility is constant over an order of magnitude variation of time (3–24 h). The anomalously low SnO_2 values in glass immediately adjacent to the cassiterite crystal, discussed above, is attributed to a lower solubility in a more peraluminous melt. However, the lack of time dependence indicates that this affect does not interfere with the determination of solubility.

Tin Diffusion

The diffusion coefficients determined in this study, reported as SnO_2, are summarized in Table 1 and Fig. 5. At reduced conditions, the reproducibility is better than ±0.5 log units (cm^2/s). In the most oxidized experiments, the diffusion coefficients are less accurate, owing to greater errors in the determination of low SnO_2 concentrations and fewer points defining the diffusion profiles. In one experiment (samples Sn2-1 and Sn2-2), the pressure was erroneously released before the complete cooling of the samples, resulting in vesiculation and expansion of the capsules. Although this error did not affect the determination of the solubilities, the diffusion coefficients are not meaningful, and thus, were excluded from the data. The fastest diffusion rate measured, $\sim 10^{-8}$ cm^2/s, corresponds to the most reduced experiment and there is an apparent decrease in SnO_2 diffusivity, with increasing f_{O_2}, with the most oxidized experiment yielding a diffusion rate of $\sim 10^{-9}$ cm^2/s.

DISCUSSION

Comparison with Previous Solubility Studies

It is difficult to compare our results with the compilation of Štemprok (1990), owing to a lack of information on melt composition and redox conditions. However, the work of Ryabchikov et al. (1978) is cited as having obtained SnO_2 solubilities of 1300–2600 ppm for an f_{O_2} range of Fe_2O_3-Fe_3O_4 to Ni-NiO at 750°C and 1.5 kbar for a haplogranite composition (the latter represented by the open circle on Fig. 2). Our experiments indicate solubilities of approximately 800–3000 ppm SnO_2 over a similar f_{O_2} range, and thus, agree with Ryabchikov et al. (1978). The vapor-melt partition and solubility study of Taylor and Wall (1992) was conducted over a log f_{O_2} range of approximately FMQ−1 to FMQ+1.4. Since their data indicate an apparent dependence of SnO_2 solubility in the silicate melt on the Cl abundance of the aqueous phase, only the Cl-free data are compared with this study. There is an excellent agreement between our data and those of Taylor and Wall (1992) for f_{O_2} conditions higher than the Ni-NiO buffer (Fig. 2). By contrast, at increasingly more reduced conditions, we find increasingly higher SnO_2 solubilities and, at the Co-CoO buffer, the experiments of Taylor and Wall (1992) indicate a solubility that is one order of magnitude lower than this study. The small differences in temperature and composition of the two studies cannot account for this discrepancy.

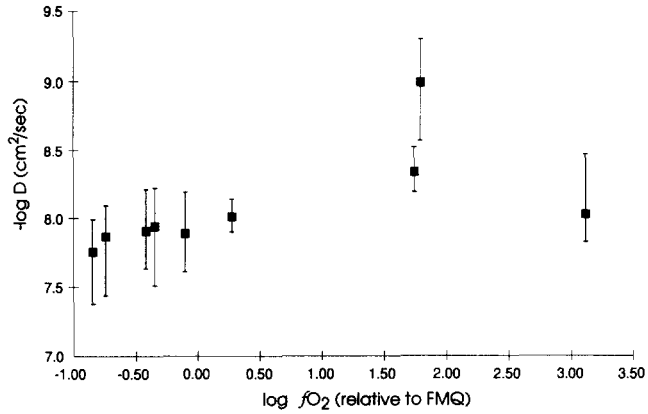

FIG. 5. Cassiterite solubility (as log ppm SnO_2) vs. the average diffusion coefficient of SnO_2. Note that high SnO_2 concentrations correspond to low f_{O_2} conditions. The error bars represent the range of diffusivities calculated from each experiment.

Concerning the potential errors in this study, in the most reduced experiments the estimated error on f_{H_2} measurements is ±1 bar, which results in an log f_{O_2} error of approximately ±0.1. A difference of −1 log unit f_{O_2} (which is still too small to explain the difference with the results of Taylor and Wall, 1992) requires, using experiment Sn1 as an example, a H_2 fugacity of approximately 140 bars instead of the measured 44 bars; such a large error is highly improbable. Another potential source of error is the H_2O content of the melt. Since our experiments were H_2O-undersaturated, the wt% H_2O loaded in the capsule should be the H_2O content of the melt, and comparable major-element totals of the experiment glasses and the 6.0 wt% H_2O secondary glass standard indicate that our H_2O content estimates are reasonable. In addition, the H_2O content of the most reduced experiment was determined by infrared spectroscopy using a Nicolet FTIR 710 spectrometer equipped with a Nicplan microscope. The local resolution was approximately 50 μm; the heights of the absorption bands near 4500 and 5200 cm^{-1} were measured and linear molar absorptivities were taken to be 1.83 and 1.7, respectively, and a glass density of 2.3 g/cm^3 was used for the calculation of the H_2O content. The value obtained is 5.8 wt% H_2O, which compares favourably to the 5.4 wt% measured by weight difference. Finally, the lack of time dependence on solubility and diffusion, and the excellent fit of the data to theoretical diffusion profiles indicate that the diffusion method is accurate for determining solubility.

Before examining the potential errors in the study of Taylor and Wall (1992), it is important to note that similar experimental equipment was used (i.e., IHPV equipped with a Shaw membrane); thus, the errors associated with estimating the f_{H_2} and f_{O_2} in the pressure vessel are similar to this study. The most important difference in the methodology of the two studies is that in this work, cassiterite solubility is calculated by measuring diffusion profiles in glasses, whereas in the former study it was determined by measuring Sn contents of homogeneous glasses. In the approach of Taylor and Wall (1992), Sn diffused into the walls of the Au capsule and produced oxygen:

$$SnO(\text{melt or fluid}) = 0.5\ O_2(\text{melt or fluid}) + Sn(\text{Sn-Au alloy}); \quad (4)$$

$$SnO_2(\text{melt, fluid or crystal}) = O_2(\text{melt or fluid}) + Sn(\text{Sn-Au alloy}). \quad (5)$$

Tin alloy reactions could control or modify f_{O_2}; however, these reactions cannot be used to calculate f_{O_2} without knowledge of the activities of tin in the melt or in alloys with Au, which are currently unknown. Alternatively, the activity of SnO_2 in the alloy could control or modify the activity of SnO_2 in the silicate liquid. In the most reduced experiments of Taylor and Wall (1992), the amount of Sn in the alloy is an order of magnitude greater than that in the silicate glass, but the alloy is heterogeneous (0 to >15 wt% Sn, cf. Taylor, 1979). Equilibrium between cassiterite, silicate melt and Sn-Au alloy was, therefore, not attained. For a Sn-Au alloy with >0.2 wt% Sn, the Sn in the alloy diffuses at the same rate or slightly faster (Herzig and Heumann, 1972) than Sn in a haplogranitic liquid. In an equilibrium experiment, equilibration is attained via diffusion, but since Sn is being lost from the melt at roughly the same rate as it is being added, the silicate liquid cannot be saturated with respect to cassiterite until the alloy at the melt interface also has reached equilibrium. We attempted to replicate the results of Taylor and Wall (1992) in one experiment (conditions of Sn12, Table 1). Roughly equal weight proportions of cassiterite crystals, haplogranite gel, and water were loaded into a single Au capsule and welded shut (this differs from the former study where a crimped double-capsule method was employed). In this experiment, Sn diffused through the capsule wall, creating a hole in less than two days (indicating liquid Au-Sn with a minimum Sn content of 7.6 wt%; Legendre et al., 1987), confirming that alloying is a serious problem at reduced conditions. We suggest that the data of Taylor and Wall (1992) at reduced conditions reflect either higher f_{O_2} or reduced SnO_2 activity in the melt, as a consequence of alloying. By contrast, at oxidized conditions, Sn alloying is not a problem and cassiterite solubility is independent of f_{O_2} (discussed below); hence, their results are similar to this study.

Speciation and Diffusion of Tin in Haplogranitic Melt

With increasingly oxidized conditions the Sn^{2+}/Sn^{4+} ratio of the melt will diminish and above a certain f_{O_2} value, cassiterite solubility will be independent of f_{O_2} (reaction 6; represented schematically by the inset in Fig. 2).

$$SnO_2(\text{crystal}) = SnO_2(\text{melt}); \quad (6)$$

$$SnO_2(\text{crystal}) = SnO(\text{melt}) + 0.5\ O_2(\text{melt}). \quad (7)$$

At the *P-T* and composition of this study, this independence occurs at a log f_{O_2} value higher than approximately FMQ+1.5. By contrast, the strong increase of SnO_2 solubility with decreasing f_{O_2} (at log f_{O_2} values < FMQ+0.27) indicates that significant tin dissolved into the melt as Sn^{2+} at more reduced conditions. If, at reduced conditions γSn^{2+}(melt) is constant, the relationship between log Sn concentration (total Sn as Sn^{2+}) and log f_{O_2} will define a slope of −0.5 (reaction 7). We do not exclude the possibility that γSn^{2+}(melt) changes with Sn concentration (non-Henrian behaviour). However, the slope on Fig. 2 for the reduced experiments is nearly −0.5, and therefore, we conclude that cassiterite dissolved dominantly as Sn^{2+} in these experiments.

There are relatively few diffusion studies that can be compared directly to this study. In terms of comparable major-element composition and water content, the most relevant are those of Harrison and Watson (1983, 1984), Rapp and Watson (1986), and Pichavant et al. (1992). By extrapolating the 6 wt% H_2O data of these studies to 850°C, the diffusion of Sn at reduced conditions is similar to that of Ca (log D − 8.7 cm^2/s), 1.5 orders of magnitude faster than Zr (log D −10.5 cm^2/s), two orders of magnitude faster than P (log D −10.7 cm^2/s), and four orders of magnitude faster than REEs (log D −12 cm^2/s). Using the data of Zhang et al. (1991), it can also be estimated that Sn, in haplogranitic melt with roughly 6 wt% H_2O, diffuses approximately one order of magnitude slower than H_2O. The apparent decrease in the diffusion coefficient of tin with increasing f_{O_2}, together with the decrease in solubility, is consistent, with Sn^{2+} behaving as a network modifier at reduced conditions, whereas Sn^{4+} has a higher coordination number and behaves as a HFSE at oxidized conditions. For the reduced conditions, this is supported by the fact that cassiterite dissolution is accompanied by alkali, and not silica diffusion.

A disadvantage of the experimental method of the current study is that the diffusion profiles produced are not amenable to analysis by Mossbauer spectroscopy, and without knowledge of the Sn^{2+}/Sn^{4+} ratio, the activity coefficients of tin cannot be directly calculated. However, one possible solubility model is that at a given redox state, there is a Sn^{2+} and Sn^{4+} saturation value, dependent on coordination. If we assume that the Sn^{4+} saturation value is independent of f_{O_2}, the implied Sn^{2+}/Sn_{total} ratios of the current study range from nearly 0 at log f_{O_2} values > FMQ+1.5 to 0.97 for the most reduced experiment (FMQ−0.84). This contrasts strongly with the Mossbauer spectroscopic analyses in Taylor and Wall (1992), where at FMQ−0.84, a Sn^{2+}/Sn_{total} ratio of roughly 0.5 is indicated. We question the validity of this ratio, in light of the differences in SnO_2 solubility discussed above. This is supported by the fact that in the controlled atmosphere experiments of Johnston (1965) the Sn^{2+}/Sn_{total} ratio (determined by titration) in dry $Na_2O \cdot 2SiO_2$ melts at 1085°C ranged from <0.01 at FMQ+5 to 0.8 at FMQ−1. However, the question of Sn^{2+}/Sn^{4+} ratios in silicate melts cannot be resolved without further experimentation.

Implications

Granite-related tin deposits are commonly considered to have had a redox state between those of the FMQ and Ni-NiO buffers (Dubessy et al., 1987); thus the f_{O_2} range in this study is directly applicable to natural studies. Considering first partial melting processes, it is evident that for a crustal source (2–10 ppm Sn, Lehmann, 1990), a granitic melt will be greatly undersaturated with respect to cassiterite, regardless of the f_{O_2} conditions. It follows that for a granitic liquid to be subsequently saturated with cassiterite, Sn must be strongly incompatible and a high degree of fractional crystallization is required. Evidence that such processes are naturally occurring

is provided by Ongonites, which contain up to 500 ppm Sn (Antipin et al., 1981) and the Macusani glasses, which contain up to 194 ppm Sn, Pichavant et al. (1988). The evaluation of Sn(melt) contents from Sn-granites is more complicated since whole-rock analyses are not representative of melt compositions and must be interpreted as cumulates. In the study of the Nong Sua aplite-pegmatite system, Linnen et al. (1992), based on whole-rock Sn determinations and mineral melt partition coefficients, concluded that a cassiterite-free graphic quartz-K-feldspar layer with 40 ppm Sn crystallized from a melt that contain on the order of 700 ppm Sn and textural evidence was presented that suggests that elsewhere in the same complex silicate melt was saturated with respect to cassiterite. In another plutonic example, Cuney et al. (1992) concluded that the high whole-rock Sn contents of the Beauvoir granite (up to 1400 ppm Sn; with disseminated cassiterite) cannot be explained by hydrothermal remobilization and that the melt was saturated with cassiterite.

In the latter examples, the f_{O_2} is interpreted to have increased during the late magmatic to early hydrothermal stages and specifically for Nong Sua, from approximately FMQ to Ni-NiO (Linnen and Williams-Jones, 1993; Cuney et al., 1992). It is also important to note that the solidus temperature at Nong Sua is interpreted to have been approximately 650°C (Linnen and Williams-Jones, 1993) and at Beauvoir was experimentally determined to have been <600°C (Pichavant et al., 1987). Cassiterite solubility in silicate melts is almost certainly temperature dependent (Štemprok, 1990); thus, the silicate liquid (±fluid phase) in these natural examples probably reached cassiterite saturation below the 800 ppm SnO_2 solubility determined in this study, at f_{O_2} > Ni-NiO and 850°C (although conversely B, Li, F, etc., might increase SnO_2 solubility). It is clear from the experimental work that a late stage increase of f_{O_2} is an effective mechanism for cassiterite crystallization from a highly evolved granitic melt.

In terms of broader applications, the use of the behaviour of Sn is not restricted to granitic rocks and can also be employed to basalt petrogenesis and the evolution of the Earth, e.g., Jochum et al. (1993). The strong f_{O_2} dependence of tin solubility demonstrated in this study suggests that Sn analyses, in any magmatic series, might prove useful as a marker of changes in the redox state of melts.

Acknowledgments—We are grateful to R. Helbig for supplying us with synthetic cassiterite crystals, for discussions with B. Scaillet, and to O. Rouer for help with the electron microprobe analyses. This study was supported by a Natural Science and Engineering Research Council of Canada postdoctoral fellowship to R. L. L. and a grant to S. B. from the University of St. Andrews, and by the CNRS program "métallogénie". Reviews by D. Baker, P. Candela, and D. London improved the manuscript, but the content of this paper is solely the responsibility of the authors.

Editorial handling: P. C. Hess

REFERENCES

Ancey M., Bastenaire F., and Tixier R. (1978) Applications des méthodes statistiques en microanalyse. In *Microanalyse et Microscopie Electronique à Balayage*, pp. 323–347. Les Éditions de Physique, Orsay.

Antipin V. S., Kovalenko V. I., Kuznetsova A. I., and Persikova L. A. (1981) Distribution coefficients for tin and tungsten in ore-bearing acid igneous rocks. *Geochem. Internatl.* **18,** 92–106.

Burnham C. W. (1979) The importance of volatile constituents. In *The Evolution of Igneous Rocks: Fiftieth Anniversary Perspectives* (ed. H. S. Yoder), pp. 439–482. Princeton Univ. Press.

Chou I.-M. (1978) Oxygen buffer and hydrogen sensor techniques at elevated pressures and temperatures. In *Hydrothermal Experimental Techniques* (ed. G. C. Ulmer and H. L. Barnes), pp. 61–99. Wiley.

Cuney M., Marignac C., and Weisbrod A. (1992) The Beauvoir topaz-lepidolite albite granite (Massif Central, France): The disseminated magmatic Sn-Li-Ta-Nb-Be mineralization. *Econ. Geol.* **87,** 1766–1794.

Dubessy J. et al. (1987) Physical and chemical controls (f_{O_2}, T, pH) of the opposite behaviour of U and Sn-W as examplified by hydrothermal deposits in France and Great Britain, and solubility data. *Bull. Mineral.* **110,** 261–281.

Haar L., Gallagher J. S., and Kell G. S. (1984) *NBS/NRS Steam Tables. Thermodynamic and Transport Properties and Computer Programs for Vapor and Liquid States of Water in SI Units.* Hemisphere Publ. Co.

Harrison T. M. and Watson E. B. (1983) Kinetics of zircon dissolution and zirconium diffusion in granitic melts of variable water content. *Contrib. Mineral. Petrol.* **84,** 66–72.

Harrison T. M. and Watson E. B. (1984) The behavior of apatite during crustal anatexis: Equilibrium and kinetic considerations. *Geochim. Cosmochim. Acta* **48,** 1467–1477.

Herzig Chr. and Heumann Th. (1972) Diffusion un Korrelation in goldreichen Gold-Zinn-Mischkristallen. *Z. Naturforsch.* **27a,** 1109–1118.

Holtz F., Pichavant M., Barbey P., and Johannes W. (1992a) Effects of H_2O on liquidus phase relations in the haplogranite system at 2 and 5 kbar. *Amer. Mineral.* **77,** 1223–1241.

Holtz F., Behrens H., Dingwell D. B., and Taylor R. (1992b) Water solubility in aluminosilicate melts of haplogranite composition at 2 kbar. *Chem. Geol.* **96,** 289–302.

Ishihara S. (1981) The granitoid series and mineralization. *Econ. Geol.* 75th Anniv. Vol. pp. 458–484.

Jackson N. J., Halliday A. N., Sheppard S. M. F., and Mitchell J. G. (1982) Hydrothermal activity in the St Just mining district. In *Metallization Associated with Acid Magmatism* (ed. A. M. Evans), pp. 137–179. Wiley.

Jochum K. P., Hofmann A. W., and Seufert H. M. (1993) Tin in mantle-derived rocks: Constraints on Earth evolution. *Geochim. Cosmochim. Acta* **57,** 3585–3595.

Johnson J. W., Oelkers E. H., and Helgeson H. C. (1992) SUPCRT92 A software package for calculating the standard molal thermodynamic properties of minerals, gases, aqueous species, and reactions from 1 to 5000 bars and 0° to 1000°C. *Comp. Geosci.* **18,** 899–947.

Johnston (1965) Oxidation-reduction equilibria in molten $Na_2O \cdot 2SiO_2$ glass. *J. Amer. Ceram. Soc.* **48,** 184–190.

Keppler H. and Wyllie P. J. (1991) Partitioning of Cu, Sn, Mo, W, U, and Th between melt and aqueous fluid in the systems haplogranite–H_2O–HCl and haplogranite–H_2O–HF. *Contrib. Mineral. Petrol.* **109,** 139–150.

Legendre B. et al. (1987) Contribution towards clarification of Au-Sn phase diagrams for Sn contents <25 atm. %. *Mat. Sci. Tech.* **3,** 875–876.

Lehmann B. (1990) *Metallogeny of Tin.* Springer-Verlag.

Linnen R. L. and Williams-Jones A. E. (1993) The evolution of pegmatite-hosted tin-tungsten mineralization at Nong Sua, Thailand: Evidence from fluid inclusions and stable isotopes. *Geochim. Cosmochim. Acta* **57,** 735–747.

Linnen R. L., Williams-Jones A. E., and Martin R. F. (1992) Evidence of magmatic cassiterite mineralization at the Nong Sua aplite-pegmatite complex, Thailand. *Can. Mineral.* **30,** 739–761.

Naski G. G. and Hess P. C. (1985) SnO_2 solubility: experimental results in peraluminous and peralkaline high silica glasses. *EOS* **66,** 412.

Persikov E. S., Zharikov V. A., Bukhtiyarov P. G., and Pol'skoy S. F. (1990) The effect of volatiles on the properties of magmatic melts. *Eur. J. Mineral.* **2,** 621–642.

Pichavant M. (1987) Effects of B and H_2O on liquidus phase relations in the haplogranite system at 1 kbar. *Amer. Mineral.* **72,** 1056–1070.

Pichavant M., Boher M., Stenger J. F., Aïssa M., and Charoy B. (1987) Relations de phase des granites de Beauvoir à 1 et 3 kbar, en condition de saturation en H_2O. *Géologie France* **2–3,** 77–86.

Pichavant M. et al. (1988) The Miocene-Pliocene Macusani volcanics, SE Peru. *Contrib. Mineral. Petrol.* **100,** 325–338.

Pichavant M., Montel J.-M., and Richard L. R. (1992) Apatite solubility in peraluminous liquids: Experimental data and an extension of the Harrison-Watson model. *Geochim. Cosmochim. Acta* **56,** 3855–3861.

Rapp R. P. and Watson E. B. (1986) Monazite solubility and dissolution kinetics: implications for the thorium and light rare earth chemistry of felsic magmas. *Contrib. Mineral. Petrol.* **94,** 304–316.

Robie R. A., Hemingway B. S., and Fisher J. J. (1979) *Thermodynamic Properties of Minerals and Related Substances at 298.15 K and 1 bar (10^5* Pascals*) Pressure and at Higher Temperatures; USGS Bull.* **1452.**

Ryabchikov I. D., Durasova N. A., Barsukov V. L., and Efimov A. S. (1978) Oxidation-reduction potential as factor of an ore-bearing capacity of acid magmas. *Geokhimiya* **8,** 1243–1246 (in Russian).

Scaillet B., Pichavant M., Roux J., Humbert G., and Lefèvre A. (1992) Improvements of the Shaw membrane technique for measurement and control of f_{H_2} at high temperatures and pressures. *Amer. Mineral.* **77,** 647–655.

Štemprok M. (1990) Solubility of tin, tungsten and molybdenum oxides in felsic magmas. *Mineral. Deposita* **25,** 205–212.

Taylor J. R. P. (1988) Experimental studies on tin in magmatic-hydrothermal systems. Ph.D. thesis, Monash Univ., Australia.

Taylor J. R. P. and Wall V. J. (1992) The behaviour of tin in granitoid magmas. *Econ. Geol.* **87,** 403–420.

Thiel B. and Helbig R. (1976) Growth of SnO_2 single crystals by a vapour phase reaction method. *J. Cryst. Growth* **32,** 259–264.

Webster J. D. and Holloway J. R. (1988) Experimental constraints on the partitioning of Cl between topaz rhyolite and H_2O and H_2O + CO_2 fluids: New implications for granitic differentiation and ore deposition. *Geochim. Cosmochim. Acta* **52,** 2091–2105.

Zhang Y., Stolper E. M., and Wasserburg G. J. (1991) Diffusion of water in rhyolitic glasses. *Geochim. Cosmochim. Acta* **55,** 441–456.